

PAPER: Interdisciplinary statistical mechanics

Minimization of spatial cover times for impaired self-avoiding random walks: the mirage effect

Daniel Campos*, Javier Cristín and Vicenç Méndez

Grup de Física Estadística, Departament de Física, Facultat de Ciències,
Universitat Autònoma de Barcelona, 08193 Bellaterra (Barcelona) Spain
E-mail: daniel.campos@uab.cat

Received 24 February 2021

Accepted for publication 30 April 2021

Published 11 June 2021



Online at stacks.iop.org/JSTAT/2021/063404
<https://doi.org/10.1088/1742-5468/ac02b8>

Abstract. Self-avoidance is a common mechanism to improve the efficiency of a random walker for covering a spatial domain. However, how this efficiency decreases when self-avoidance is impaired or limited by other processes has remained largely unexplored. Here we provide a numerical study in regular lattices for the case when the self-avoiding signal left by a walker both (i) saturates after successive revisits to a site, and (ii) evaporates, or disappears, after some characteristic time. We surprisingly reveal that the mean cover time becomes minimum for intermediate values of the evaporation time, leading to the existence of a nontrivial optimum management of the self-avoiding signal. We show that this is a consequence of a complex dynamics arising from the interplay between signal evaporation and signal saturation, in which evaporation has the capacity of creating some sort of *mirages* (sites or regions that the walker see as unvisited, though in fact they are not) that enhance the searcher mobility, so contributing to a more efficient exploration of the lattice that counteracts the effects of signal saturation. Remarkably, we argue both through scaling arguments and from numerical results, that this *mirage effect* will become more and more significant as long as the domain size increases.

Keywords: stochastic search, self-propelled particles, stochastic processes

*Author to whom any correspondence should be addressed.

Contents

1. TSAW with signal saturation	4
2. TSAW with signal evaporation	5
2.1. Case without saturation ($\gamma = 0$)	6
2.2. Case with perfect saturation ($\gamma = \infty$)	7
2.3. General case	10
3. Discussion	12
Acknowledgments	13
References	13

Four decades ago, Pierre Gilles De Gennes coined the suggestive expression *ant in the labyrinth* to describe movement through disordered systems [1]. It is widely known that by introducing obstacles in regular lattices the effective diffusion coefficient of random walkers gets reduced proportionally, and eventually transport becomes subdiffusive when the percolation threshold is reached due to the self-similar properties of the underlying structure [2]. Despite the intrinsic complexity of the problem, throughout the years effective propagators and Fokker–Planck equations have been proposed, and its main scaling properties have been progressively revealed [3–10].

A far less understood situation, however, is that in which disorder is not quenched but dynamically generated by the trajectory itself. Some well-known models fulfilling this idea are self-avoiding or self-repelling random walks, in which revisits to previous nodes/positions are systematically avoided throughout the trajectory. So, strong non-Markovian effects govern the dynamics of these systems, which turns their analytical treatment cumbersome in most cases. Nevertheless, the interest of self-avoiding walks as stochastic processes for optimizing exploration or coverage of the media is evident, as they represent a way to consistently avoid overlaps typical of recurrent trajectories (e.g. Brownian paths), specially in low-dimensional systems.

Coverage optimization through self-avoiding rules is potentially attractive for sampling efficiently large phase spaces (for instance, for Monte Carlo algorithms in statistical mechanics) [11]. Furthermore, the concept of self-avoidance is also important to understand the dynamics of particles which are able to leave locally some kind of signal or debris which can yield a local repulsive potential afterward [12]. Such systems are gaining nowadays a renewed interest due to the growing experimental evidence that many microorganisms like bacteria or T-cells could be able to use self-signalling mechanisms for increasing their dispersal, feeding, or predation efficiencies [13–17], and also due to the availability of new techniques for generating controllable artificial self-repelling

particles in the lab, e.g. microdroplets in surfactant solutions [18, 19]. Finally, self-avoidance can be seen as a mechanism for optimizing searches, for instance during animal exploration/foraging [20–24] or in search algorithms through the internet [25–30] or in social networks [31, 32], among other.

A reference model within this context is the true self-avoiding walk (tSAW), first introduced by Amit, Parisi and Peliti [33] as a way to disentangle self-avoiding random walks from models of polymer growth, as the latter are known to be typically self-killing instead of self-avoiding [12]. The tSAW rule of advance works as follows: given a present position of the walker, the probability to jump in the next step to each of the first neighbors j is $p_j = Z^{-1}e^{-gn_j}$, with $Z \equiv \sum_{j=1}^z e^{-gn_j}$ a normalization factor where z is the coordination number of the lattice, g a positive constant and n_j (denoted here as the signal intensity) is the number of visits that the walker has made to node j previously. Accordingly, those neighbors less visited in the past are preferentially selected, with g controlling the efficiency of the self-avoiding mechanism.

Coverage properties of classical random walks moving within regular (finite) lattices in d dimensions have been extensively explored over the last thirty years [11, 34–42]. The coverage problem in $d = 1$, for example, can be mapped to a first-passage problem and then analytical expressions can be obtained for the mean time required to cover all nodes in the domain, $\langle T_{\text{cov}} \rangle = N(N - 1)$, with N denoting the number of nodes in the lattice [34]. Also, the case $d = 2$ has been proved to satisfy $\langle T_{\text{cov}} \rangle \sim N(\log N)^2$, while for $d \geq 3$ it is found that $\langle T_{\text{cov}} \rangle \sim N(\log N)$ [37, 41]. Furthermore, universal scaling properties have been revealed recently to emerge in the distribution of coverage times for non-recurrent random walks in different dimensions [43]. An equivalent analysis for the tSAW, on its turn, becomes more complicated due to the memory effects involved. Still, we know that for $d = 1$ an asymptotic scaling $\langle T_{\text{cov}} \rangle \sim N^{3/2}$ will be found, while transiently the self-avoiding mechanism will result in a ballistic motion (so $\langle T_{\text{cov}} \rangle \sim N$ for smaller N). For $d = 2$, on its turn, the scaling $\langle T_{\text{cov}} \rangle \sim N(\log N)$ for large g has been conjectured in [25] and confirmed numerically in [12]. Also, since the critical dimension of the tSAW is known to be $d = 2$ [33], the scaling is expected to be identical to that of regular random walks for $d > 2$.

Despite all these findings, there are very few works in the literature that have explored how the properties of these models get modified when self-avoidance is limited and/or impaired (though the works in [12, 44] represent some interesting exceptions). If we consider the potential applications mentioned above (e.g. in self-repelling trajectories of microdroplets or microorganisms resulting from chemical signals) it is natural to wonder about the effects that diffusion or evaporation (among other) of these signals will have on the properties of the corresponding trajectories, and on their coverage efficiency. This idea has been addressed recently for a modified version of the tSAW introducing dispersal of the chemical through a variation of the signal levels in the neighboring nodes whenever a site is visited; this model has led to the surprising observation that tSAWs can become self-trapping in some situations [12]. Our present work offers an alternative view within this context, by exploring how tSAW coverage properties are modified if (i) the effect of the self-avoiding signal is assumed to become less and less effective as long as successive visits to a node are performed (we call this *signal saturation*), and (ii) the signal can disappear with time (we call this *signal evaporation*). As we will

show, several unexpected facts arise as a consequence of these restrictions. In particular we observe that increasing the rate of *evaporation* does not always result in a larger coverage time, but an optimal *evaporation* time can exist for systems below the critical dimension of the tSAW. This effect, as we shall see, is modulated by the intensity of the *signal saturation*, and its significance increases as long as the size of the system grows.

1. TSAW with signal saturation

First of all, we implement the idea of *signal saturation* by considering that the signal intensity is of the form $n_j = \sum_i i^{-\gamma}$ (with γ a positive parameter), where the sum is carried out over all the previous visits of the walker to that site. In absence of additional effects, then, the intensity grows monotonically with the number of visits to a site and eventually saturates at $\zeta(\gamma)$, with ζ the Riemann zeta function. Then, the first visit to the site ($i = 1$) will increase the intensity in one unit while the increase will be smaller for subsequent visits. In particular, note that for $\gamma = 0$ the model with saturation recovers the classical rule of the tSAW, while in the limit $\gamma \rightarrow \infty$ the walker is only able to distinguish visited from nonvisited sites (but it cannot distinguish, or *remember*, how many times the site has been visited), so for the latter the energy landscape becomes almost homogenous when most of the sites in the lattice have been visited. Note that this $\gamma \rightarrow \infty$ case can be seen too as a particular case of the known *self-attracting random walk* model [45–47], for which β is allowed to be either positive or negative in order to turn the trajectory from self-avoiding to self-attracting.

For the 1d case, the scaling of the mean coverage time with N will exhibit a $\langle T_{\text{cov}} \rangle \sim N^{3/2}$ behavior, while $\langle T_{\text{cov}} \rangle \sim N^2$ should be expected for $\gamma \rightarrow \infty$. In 2d, similarly, $\langle T_{\text{cov}} \rangle \sim N(\log N)^\alpha$ should hold, with $\alpha = 2$ for large γ , and $\alpha = 1$ for $\gamma = 0$ [12].

The numerical results found for the mean coverage time show a monotonic increase with γ (figure 1) in 2d, making it evident that saturation precludes the walker from using all the information that was available in the classical tSAW, so that coverage becomes less and less efficient. Interestingly, for the case in 1d the behavior is no strictly monotonic but a local maximum appears for intermediate values of g . This occurs because for intermediate g there is a chance that the initial direction of motion is changed and then the walker will turn back to the region it has already visited. In such case, an intermediate value of γ will make it advance in the opposite direction to the initial one so delaying coverage significantly. Instead, for very large γ the walker will see a region with $n_j = 1$ everywhere and so motion will be isotropic and then return to the path it was following previously is easier. While this will only happen in 1d and for intermediate g , this result already suggests that the effect of the signal dynamics on the coverage efficiency is far from trivial.

Furthermore, the results reported in figure 2 confirm approximately the scaling predictions above, by showing that $\langle T_{\text{cov}} \rangle \sim N^{3/2}$ occurs for $\gamma \rightarrow 0$ and $\langle T_{\text{cov}} \rangle \sim N^2$ is recovered as $\gamma \rightarrow \infty$ in 1d. Actually, we have found that a well-behaved scaling $\langle T_{\text{cov}} \rangle \sim N^\alpha$ holds almost exactly for any γ , with $\alpha = (12 - 4\gamma)/(8 - 4\gamma)$ for $\gamma \leq 1$ and $\alpha \approx 2$ for $\gamma > 1$ providing a good fit to the numerical results. For 2d, we also find that the results fit reasonably well a scaling $\langle T_{\text{cov}} \rangle \sim N(\log N)^\alpha$, with α increasing in this case in a non-trivial fashion from 1 (for $\gamma = 0$) to 2 (which is attained for $\gamma \geq 2$).

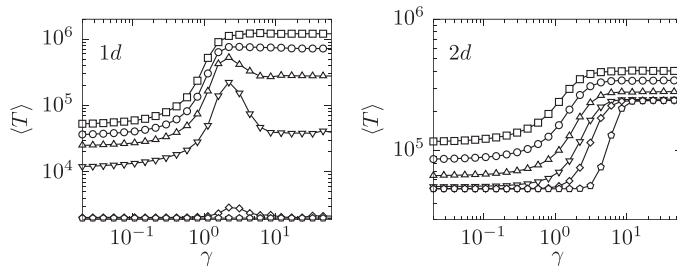


Figure 1. Mean coverage time $\langle T_{\text{cov}} \rangle$ for the tSAW model with saturation as a function of the saturation parameter γ in $d = 1$ (with $N = 2 \times 10^3$) and $d = 2$ ($N = 128 \times 128$). Plots are shown in both cases for $g = 0.5$ (squares), $g = 1$ (circles), $g = 2$ (triangles), $g = 4$ (inverted triangles), $g = 10$ (diamonds) and $g = 10^2$ (pentagons).

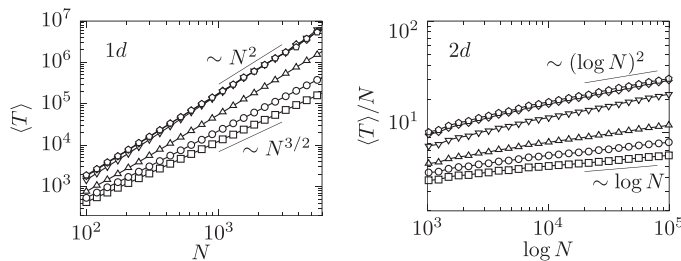


Figure 2. Mean coverage time normalized with respect to the case $\gamma = 0$, $\langle T \rangle$ for the tSAW model with saturation as a function of the domain size N . Plots are shown in both cases for $\gamma = 0$ (squares), $\gamma = 0.5$ (circles), $\gamma = 1$ (triangles), $\gamma = 2$ (inverted triangles), $\gamma = 4$ (diamonds) and $\gamma = 100$ (pentagons). In all cases $g = 1$ has been used.

As a complementary result, one can study the behavior of the survival fraction $S(t)$, it is, the mean fraction of sites that remain yet unvisited by time t . This is presented in figure 3. Interestingly, for tSAW the decay of the survival fraction is known to be faster than exponential (since the energy landscape always tends to drive the walker toward unvisited regions), while regular random walks show a slower-than-exponential decay (as the rate at which unvisited sites are found decays with the number of these sites that are still available) followed by an asymptotic exponential decay (when less than one site in average is available). In consonance with this, figure 3 shows a transition from one behavior to the other. So, for γ small the decay is faster than exponential even for large times. However, for γ large enough, $S(t)$ decays faster than an exponential only for short times (as long as self-avoidance governs the system) but then the decay becomes much slower as saturation effects become apparent, both in 1d and 2d.

Note that all these results (and those coming in the next sections, we advance) are only presented for 1d and 2d lattices. We have checked that for walks above the critical dimension of the classical TSAW, both saturation and evaporation of the signal has a minor effect, as scaling properties of the tSAW and regular random walks are the same. Then, for $d > 2$ all the processes and results discussed in our paper become rather trivial.

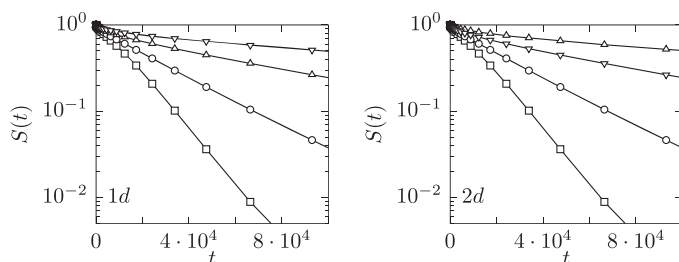


Figure 3. Average fraction of unvisited sites as a function of time for the model with saturation in $d = 1$ (with $N = 10^3$) and $d = 2$ ($N = 181 \times 181$). Plots are shown in both cases for $\gamma = 0$ (squares), $\gamma = 0.5$ (circles), $\gamma = 1$ (triangles) and $\gamma = 100$ (inverted triangles). In all cases $g = 1$ has been used.

2. TSAW with signal evaporation

Now we introduce into our model *signal evaporation*, such that the energy intensity at a site, n_i , does not only increase as a result of visiting the site, but also decreases spontaneously with time, so mimicking a loss of the signal and/or a vanishing memory of the walker. This should be implemented by decreasing the self-avoiding signal intensity n_j at every site j at a given rate. However, in order to simplify computational work we consider here an all-or-nothing rule in which a random time t_j (according to an exponential probability distribution function, $\rho(t_j) = \tau^{-1}e^{-t_j/\tau}$) is chosen whenever the walker visits a given site j , and the signal intensity n_j at that node is reset to zero at a time t_j after the visit. The parameter τ then represents the characteristic timescale at which the memory of the signal is completely lost by the effect of *evaporation*. While all the results reported in the following have been obtained through this all-or-nothing rule, the numerical analysis reveal that our conclusions would remain qualitatively the same if a progressive *evaporation* rate proportional to $\sim \tau^{-1}$ was considered instead.

2.1. Case without saturation ($\gamma = 0$)

First we study the classical tSAW (without saturation) when evaporation of the signal is introduced. By examining the mean cover time as a function of the characteristic evaporation time τ (figure 4) we observe in most of the cases a monotonic decay, which means that the main effect of evaporation is to destroy part of the information collected through the self-avoiding mechanism, and then a fast evaporation (i.e. small τ) is detrimental for the efficiency of coverage.

However, intermediate values of τ for large g in 1d represents an exception, and show that transiently evaporation can benefit the coverage process. This intriguing result will be extended and discussed in detail in the cases below.

On the other side, the effect on the survival fraction $S(t)$ in this case is slightly different (figure 5), if compared to that above in figure 3. While at intermediate times self-avoidance can be exploited by the walker and so the decay is faster than exponential, asymptotically the signal evaporation makes that older information from the path gets lost, so the walker is only able to avoid its more recent path. Then, some

Minimization of spatial cover times for impaired self-avoiding random walks: the mirage effect

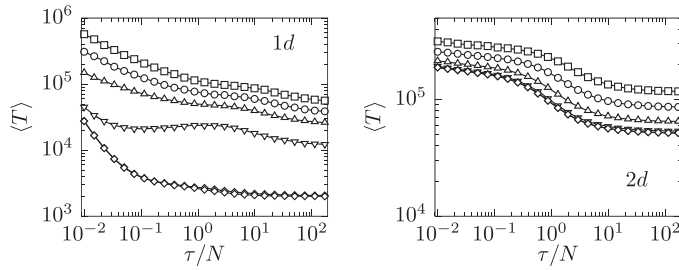


Figure 4. Mean coverage times for the model with evaporation (without saturation) as a function of the relative evaporation time τ/N in $d = 1$ (with $N = 2 \times 10^3$) and $d = 2$ ($N = 128 \times 128$). Plots are shown in both cases for $g = 0.5$ (squares), $g = 1$ (circles), $g = 2$ (triangles), $g = 4$ (inverted triangles), $g = 10$ (diamonds) and $g = 10^2$ (pentagons).

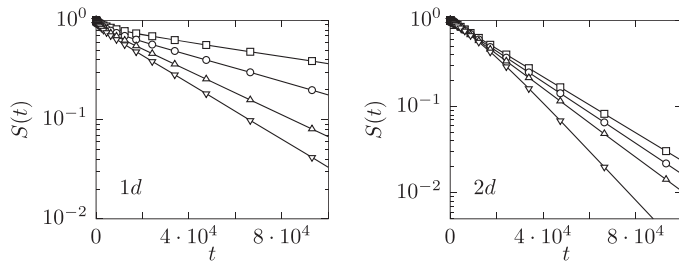


Figure 5. Average fraction of unvisited sites as a function of time for the model with evaporation (without saturation) in $d = 1$ (with $N = 10^3$) and $d = 2$ ($N = 128 \times 128$). Plots are shown in both cases for $\tau/N = 10^{-2}$ (squares), $\tau/N = 0.2$ (circles), $\tau/N = 4$ (triangles), $\tau/N = 100$ (inverted triangles). In all cases $g = 1$ has been used.

kind of persistent trajectory emerges and the decay is approximately exponential (but not faster-than-exponential as for $\gamma = 0$ in figure 3), as expected for persistent random walks [43].

2.2. Case with perfect saturation ($\gamma = \infty$)

The situation becomes much more complex when both processes, saturation and evaporation, are put together. First, we explore the role of evaporation for the extreme case of perfect saturation ($\gamma = \infty$). In this situation, after a time of the order of N a relatively large region of the lattice has been covered, and the saturation will gradually lead to a homogenous energy landscape, which is highly uninformative for the walker. In that situation, paradoxically, evaporation of the signal could be advantageous for coverage since it will introduce some sort of heterogeneity within the landscape. Although having a random nature, this heterogeneity could enhance the walker mobility toward regions that are (only apparently) unvisited, so we could term this as a *mirage* effect.

The movement toward these *mirage* regions favored by signal evaporation certainly has the potential capacity to increase the coverage efficiency. In consequence, we observe

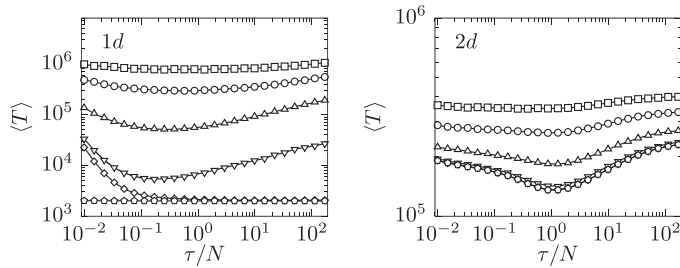


Figure 6. Mean coverage times for the model with evaporation and perfect saturation as a function of the relative evaporation time τ/N in $d = 1$ (with $N = 10^3$) and $d = 2$ ($N = 128 \times 128$). Plots are shown in both cases for $g = 0.5$ (squares), $g = 1$ (circles), $g = 2$ (triangles), $g = 4$ (inverted triangles), $g = 10$ (diamonds) and $g = 10^2$ (pentagons).

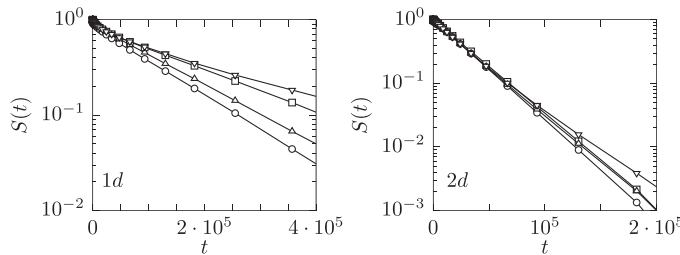


Figure 7. Average fraction of unvisited sites as a function of time for the model with evaporation and perfect saturation in $d = 1$ (with $N = 10^3$) and $d = 2$ ($N = 128 \times 128$). Plots are shown in both cases for $\tau/N = 10^{-2}$ (squares), $\tau/N = 0.2$ (circles), $\tau/N = 4$ (triangles), $\tau/N = 100$ (inverted triangles). In all cases $g = 1$ has been used.

that the dependence of the mean cover time $\langle T_{\text{cov}} \rangle$ on τ is no longer monotonic but exhibits a minimum for an intermediate evaporation time which is of the order of N , as reported in figure 6. This confirms that, once self-avoidance has been exploited during a first exploration throughout the regions of the domain, the unvisited spots remaining are easier to reach by creating those *mirages* that prevent the walker from moving diffusively without any information available.

The corresponding behavior of $S(t)$ clearly confirms this view. As can be seen in figure 7, for small values of τ (it is, fast evaporation) the decay is close to exponential, in accordance to the discussion in the previous section. As τ increases the characteristic decay rate increases too (since self-avoidance is kept for longer times) and so the survival fraction decays faster.

On the contrary, for τ much higher than the characteristic size of the domain, N , the dynamics at long times changes and the survival fraction decays slower than exponential (since the energy landscape has become almost homogenous and so it can barely provide any useful information to the walker). Then, there is an optimal value of τ for which such slower-than-exponential decay is avoided thanks to the *mirages* produced by the signal evaporation.

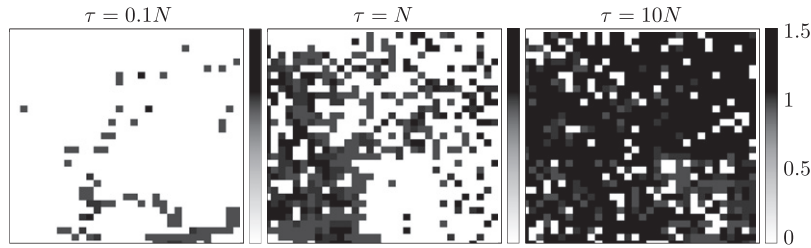


Figure 8. Signal intensity landscape for a situation close to the optimum τ_{opt} (case $\tau = N$) compared to much lower (left panel) and higher (right panel) values of τ (see labels). The maps shown correspond to a particular realization of our self-avoiding model evaluated at the coverage time $t = T_{\text{cov}}$. The gray colors in the plot represent the values of n_j for each node i in a 32×32 lattice, according to the legend on the right. The values of the parameter $g = 2$ and $\gamma = 3$ have been used in all cases.

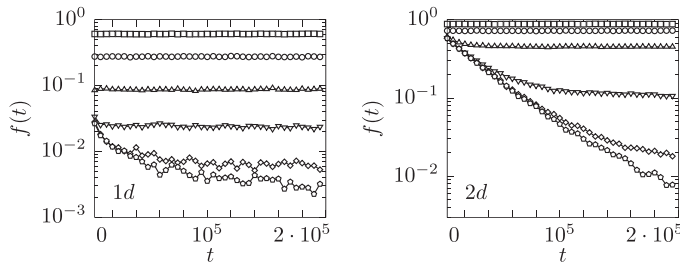


Figure 9. Fraction of *informed* decisions (see text for details) made by the walker as a function of time in $d = 1$ (with $N = 10^3$) and $d = 2$ ($N = 128 \times 128$). Plots are shown in both cases for $\tau/N = 10^{-2}$ (squares), $\tau/N = 0.1$ (circles), $\tau/N = 1$ (triangles), $\tau/N = 10$ (inverted triangles) and $\tau/N = 10^2$ (diamonds). In all the cases a value of $g = 1$ has been used.

Can we quantify, or visualize, somehow the existence of these *mirages*? This is what we try to do in figures 8 and 9. The former shows, for a particular realization of the process, the energy landscape at the instant where the coverage is finished. The left and right panels corresponds to $\tau \ll N$ and $\tau \gg N$ correspondingly, and in both cases we see large homogenous regions in the landscape which, as explained above, makes the coverage less efficient. On the contrary, for $\tau = N$, which is close to the optimal, a much more heterogenous landscape emerges, promoting the searcher mobility.

In figure 9, on its turn, we try to quantify the fraction f of *informed* decisions the searcher takes in average as a function of time. For this, we define an *informed decision* as the situation in which the intensity n_i of the first-neighbor sites (it is, those nodes to which the walker can jump in the next step) are different enough; at practice we use in figure 9 the criteria that the values of gn_j , computed for every neighbor site j , have a minimum difference of 0.1 among them. This means that the searcher sees locally significant differences in the energy landscape available, and so it can preferentially jump to some particular nodes. The behavior of the fraction f with time, again, is very different as a function of τ . For $\tau \ll N$ the fraction remains large, since evaporation is

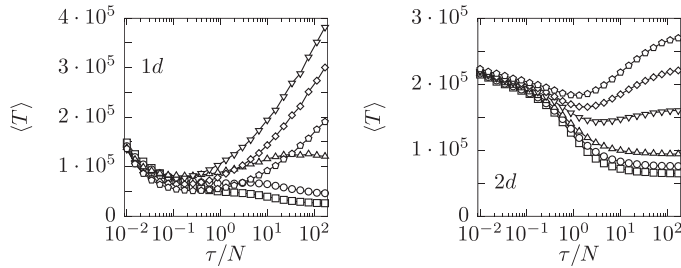


Figure 10. Mean time coverage as a function of the characteristic *evaporation* time. For $d = 1$ (upper plot) we take $N = 2 \times 10^3$ and for $d = 2N = 128 \times 128$, and show plots for $\gamma = 0$ (squares), $\gamma = 0.5$ (circles), $\gamma = 1$ (triangles), $\gamma = 2$ (inverted triangles), $\gamma = 3$ (diamonds) and $\gamma = 100$ (pentagons). In all cases $g = 2$.

fast and then (apparently) unvisited sites are always available. For $\tau \gg N$ the fraction of *informed* decisions decays continually, so the search becomes more and more blind as time goes by (note that as f becomes very small, fluctuations due to finite-size effects in the domain are observed in figure 9). For the close-to-optimal case, instead, the number of *informed* decisions decays initially with time but eventually saturates at a constant value which maintains *informed decisions* at a convenient level to enhance mobility. Though we have tried to check whether the saturation value reached by f in the optimal case satisfies any universal property or scaling, unfortunately it seems to depend much on the model parameters (g , γ and N) in a nontrivial way, so we cannot provide a more detailed quantitative description of how the energy landscape looks like in the optimal case.

2.3. General case

To complete the data from the previous section, we finally explore how the optimum τ minimizing the cover time explicitly depends on the parameters g and γ . In short, we find numerically that an optimum value of τ is found whenever saturation is fast enough and then evaporation can be useful for counteracting its effect. So that, there is a critical value of γ above which the cover time can be minimized (but note that for $\gamma = 0$ this minimization is not possible, according to the results in section 2.1). At the same time, such critical value depends explicitly on g , since this parameter also determines how accurate the self-avoiding mechanism is. Then, for larger g (very accurate self-avoidance) the critical γ increases.

Accordingly, we show the transition that occurs from monotonic decay in $\langle T_{\text{cov}} \rangle$ to the existence of an optimum τ as a function of γ (for g fixed) in figure 10. At the same time, we check that the same transition occurs at a given value of the exponent g when we keep γ fixed instead (figure 11).

Though we have exhaustively tried, it has not been possible to detect any simple scaling law that is satisfied by the system near the critical region, so we cannot characterize this behavior using phase transition theory. The properties of the critical region actually seem to depend on the system size in a highly nontrivial manner.

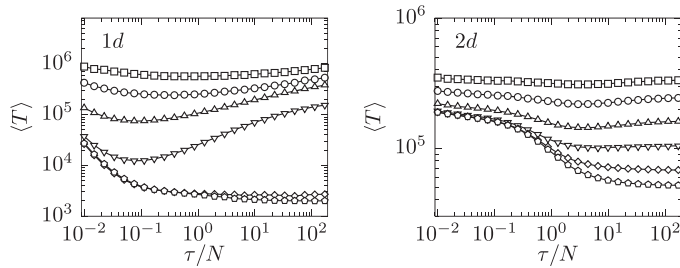


Figure 11. Mean time coverage as a function of the characteristic *evaporation* time for $\gamma = 2$. For the case $d = 1$ (upper plot) we take $N = 2 \times 10^3$, and for $d = 2$ we take $N = 128 \times 128$. Plots are shown for $\gamma = 2$ and $N = 5 \times 10^3$, and show plots for $g = 0.5$ (squares), $g = 1$ (circles), $g = 2$ (triangles), $g = 4$ (inverted triangles), $g = 10$ (diamonds) and $g = 10^2$ (pentagons).

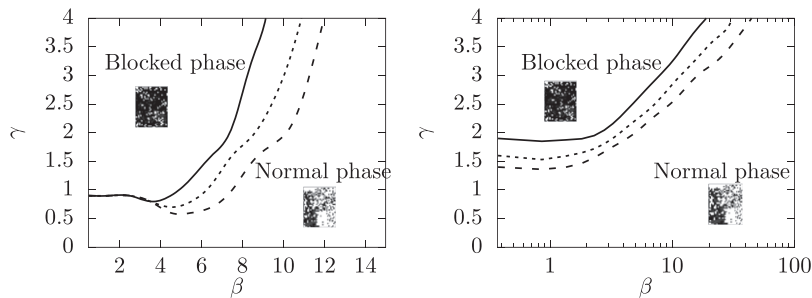


Figure 12. Phase diagram γ - g separating the ‘blocked’ phase, for which a finite τ_{opt} exists, from the normal region where it does not. The different lines correspond to different values of N : for $d = 1$ (upper plot) we plot the case for $N = 10^3$ (solid), $N = 2 \times 10^3$ (dotted) and $N = 5 \times 10^3$ (dashed). For $d = 2$ (lower plot), $N = 32 \times 32$ (solid), $N = 64 \times 64$ (dotted) and $N = 128 \times 128$ (dashed).

In order to provide at least a first guess of the properties of such optimum, it is obvious that the optimal value of τ will have an upper limit given by the condition that *mirages* cannot appear too late for being useful to the searcher; this upper limit should be of the order of $\langle T_{\text{cov}} \rangle$ (so *mirages* must appear before the cover process is complete, in average). As discussed in section 1, the dependence of $\langle T_{\text{cov}} \rangle$ on N is faster than linear (with $\langle T_{\text{cov}} \rangle \sim N^\alpha$ in 1d, with $3/2 < \alpha < 2$, and $\langle T_{\text{cov}} \rangle \sim N(\log N)^\alpha$ in 2d).

On the other side, there is also a lower limit for the optimal τ which is given by the emergence of homogenous energy landscapes in the lattice; before that happens *mirages* do not have any utility. The size of the homogenous landscapes for this to happen is, in the worst case, of the order N .

Hence, the region where *mirages* appear and can be useful to the searcher (and so the region where the optimum in τ can possibly appear) should asymptotically lie within the range $N < \tau < N^\alpha$ and $N < \tau < N(\log N)^\alpha$ for 1d and 2d, respectively. Remarkably, the size of this range increases with N , suggesting that for larger domains it should be relatively easier to observe the existence of an optimal τ . To confirm this, we show in figure 12 how the region where the optimum appears (in the g - γ phase space) increases

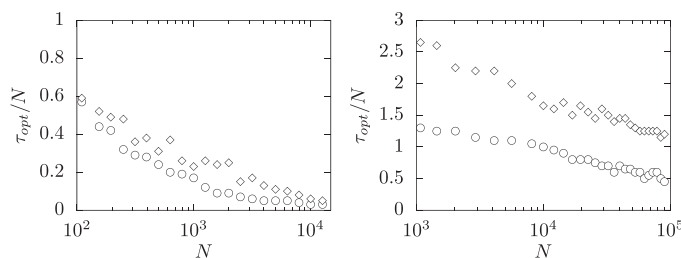


Figure 13. Optimum *evaporation* rate (rescaled according to the lattice size) in $d = 1$ (upper plot) and $d = 2$ (lower plot) as a function of the lattice size N . Two different values of the *saturation* intensity are reported: $\gamma = 2$ (circles) and $\gamma = 4$ (diamonds). $g = 10$ is used in all cases.

as a function of the domain size N . Furthermore, the specific dependence of the optimal τ on N (for constant g and γ) found numerically is sublinear, such that τ_{opt}/N seems to decay logarithmically with N (figure 13). This scaling seems to be in agreement with the range for τ mentioned above, though we cannot formally justify it in any simple manner. Anyway, we stress that this result has important implications, as in particular it would imply that $\lim_{N \rightarrow \infty} \tau_{\text{opt}}/\langle T_{\text{cov}} \rangle = 0$, so the relative evaporation time required for optimizing the coverage process would become vanishingly small for infinite domains.

3. Discussion

In summary, while self-avoidance, together with tabu searches and similar algorithms [48], is typically assumed to represent an extremely efficient mechanism for domain coverage, we have proved that when self-avoidance gets impaired by the existence of signal saturation, then evaporation of the signal can be sometimes beneficial for the coverage efficiency. This means that under certain circumstances it becomes more efficient to *forget* part of the regions previously covered that keeping full memory of the path.

This phenomenon is found to be characteristic of low-dimensional lattices, but it disappears for systems above the critical dimension of the tSAW; we have explored, in particular, all possible regions of parameters for $d = 3$ (not shown here) and have confirmed that the optimal evaporation does never appear there. Indeed, albeit all the results presented here correspond to lattices with periodic boundary conditions, the effect of considering reflecting boundaries, for example, will clearly enhance the possibility that the particle can get trapped in a region where the energy landscape is homogenous. So, this will increase the range of parameters for which an optimal τ exists. As a proof of concept, the first tests that we have carried out allow us to confirm that, at least in $d = 1$, the optimum τ can appear for reflective boundary conditions even in the absence of *signal saturation*, this is, when $\gamma = 0$ (something that does not happen for periodic boundary conditions, as we have seen in section 1).

We note that a more formal, or analytical, description of the *mirage* effect reported remains elusive yet (since we have not been able to derive any simple scaling law that should be satisfied in the nontrivial region where the optimum appears), due to the

complexity of the system. Still, we think that this novel phenomena may have interest for a wide range of situations. We note that the effect has been illustrated here for the paradigmatic case of the tSAW, but the existence of an optimal evaporation rate will presumably appear in many other self-avoiding models (e.g. in self-repelling particles or microorganisms following a vanishing chemical signal), as well as in alternative random walk models with memory. A deeper analysis of this phenomena, then, can open a useful line of research in order to promote our understanding about how the coverage efficiency of self-generated chemotaxis and/or artificial self-repelling microrobots could be enhanced. We claim that this may be not only useful for technical (e.g. pharmaceutical) applications, but can be also seen as a possible mechanism of interest for understanding navigation and/or foraging of living beings.

Acknowledgments

We thank Dr Peter Grassberger for his valuable comments and suggestions about the present work. This research has been supported by the Spanish government through Grant No. CGL2016-78156-C2-2-R.

References

- [1] De Gennes P G 1976 *Recherche* **7** 919
- [2] Bunde A and Havlin S 1991 *Fractals and Disordered Systems* (Berlin: Springer)
- [3] O’Shaughnessy B and Procaccia I 1985 *Phys. Rev. Lett.* **54** 455–8
- [4] Metzler R, Glöckle W G and Nonnenmacher T F 1994 *Physica A* **211** 13–24
- [5] Dräger J, Russ S and Bunde A 1995 *Europhys. Lett.* **31** 425
- [6] Dräger J and Bunde A 1996 *Phys. Rev. E* **54** 4596
- [7] ben-Avraham D and Bunde A 2000 *Diffusion and Reactions in Fractals and Disordered Systems* (Cambridge: Cambridge University Press)
- [8] Campos D, Méndez V and Fort J 2004 *Phys. Rev. E* **69** 031115
- [9] Bianco F, Chibbaro S, Vergni D and Vulpiani A 2013 *Phys. Rev. E* **87** 062811
- [10] Balankin A S 2015 *Phys. Rev. E* **92** 062146
- [11] Nemirovsky A M, Martín H O and Coutinho-Filho M D 1990 *Phys. Rev. A* **41** 761–7
- [12] Grassberger P 2017 *Phys. Rev. Lett.* **119** 140601
- [13] Tweedy L, Susanto O and Insall R H 2016 *Curr. Opin. Cell Biol.* **42** 46–51
- [14] Donà E *et al* 2013 *Nature* **503** 285–9
- [15] Schwab S R and Cyster J G 2007 *Nat. Immunol.* **8** 1295–301
- [16] Tweedy L, Knecht D A, Mackay G M and Insall R H 2016 *PLoS Biol.* **14** e1002404
- [17] Cremer J, Honda T, Tang Y, Wong-Ng J, Vergassola M and Hwa T 2019 *Nature* **575** 658–63
- [18] Jin C, Krüger C and Maass C C 2017 *Proc. Natl Acad. Sci. USA* **114** 5089–94
- [19] Liebchen B and Löwen H 2018 *Acc. Chem. Res.* **51** 2982–90
- [20] Berbert J M and Fagan W F 2012 *Ecol. Complex.* **12** 1–12
- [21] Sims D W, Reynolds A M, Humphries N E, Southall E J, Wearmouth V J, Metcalfe B and Twitchett R J 2014 *Proc. Natl Acad. Sci.* **111** 11073–8
- [22] Reynolds A M 2014 *Sci. Rep.* **4** 4409
- [23] Méndez V, Campos D and Bartumeus F 2014 *Stochastic Foundations in Movement Ecology* (Berlin: Springer)
- [24] Sakiyama T and Gunji Y-P 2018 *R. Soc. Open Sci.* **5** 171057
- [25] Avin C and Krishnamachari B 2008 *Comput. Netw.* **52** 44–60
- [26] Millan V M L, Cholvi V, Lopez L and Anta A F 2012 *Networks* **60** 71–85
- [27] Oshima H and Odagaki T 2012 *J. Phys. Soc. Japan* **81** 074004
- [28] Kim Y, Park S and Yook S-H 2016 *Phys. Rev. E* **94** 042309
- [29] de Arruda H F, Silva F N, Costa L d F and Amancio D R 2017 *Inf. Sci.* **421** 154–66

- [30] Herrero C P 2019 *Phys. Rev. E* **99** 012314
- [31] Gong K, Tang M, Hui P M, Zhang H F, Younghae D and Lai Y C 2013 *PLoS One* **8** e83489
- [32] Bagnato G D, Ronqui J R F and Travieso G 2018 *Physica A* **505** 1046–55
- [33] Amit D J, Parisi G and Peliti L 1983 *Phys. Rev. B* **27** 1635–45
- [34] Yokoi C S O, Hernández-Machado A and Ramírez-Piscina L 1990 *Phys. Lett. A* **145** 82–6
- [35] Aldous D J 1991 *J. Theor. Probab.* **4** 197–211
- [36] Nemirovski A M and Coutinho-Filho M D 1991 *Physica A* **177** 233–40
- [37] Brummelhuis M J A M and Hilhorst H J 1992 *Physica A* **185** 35–44
- [38] Freund H and Grassberger P 1993 *Physica A* **192** 465–70
- [39] Coutinho K R, Coutinho-Filho M D, Gomes M A F and Nemirovsky A M 1994 *Phys. Rev. Lett.* **72** 3745–9
- [40] Dembo A, Peres Y, Rosen J and Zeitouni O 2004 *Ann. Math.* **160** 433–64
- [41] Grassberger P 2017 *Phys. Rev. E* **96** 012115
- [42] Cheng K, Dong J-Q, Huang L and Yang L 2018 *Phys. Rev. E* **98** 042109
- [43] Chupeau M, Bénichou O and Voituriez R 2015 *Nat. Phys.* **11** 844–7
- [44] Moreau M, Bénichou O, Loverdo C and Voituriez R 2009 *J. Stat. Mech.* P12006
- [45] Sapozhnikov V B 1994 *J. Phys. A: Math. Gen.* **27** L151
- [46] Ordemann A, Tomer E, Berkolaiko G, Havlin S and Bunde A 2001 *Phys. Rev. E* **64** 046117
- [47] Tan Z-J, Zou X-W, Zhang W and Jin Z-Z 2001 *Phys. Lett. A* **289** 251–4
- [48] Glover F and Laguna M 1997 *Tabu Search* (Dordrecht: Kluwer)